



TIME WAITS FOR NO ONE

Enlist the experts at Bio X Cell for
Antibody Production Services

EXPLORE

RECEIVE 10% OFF NOW with code: CONTRACT22JI



Type I IFN Contributes to the Phenotype of *Unc93b1*^{D34A/D34A} Mice by Regulating TLR7 Expression in B Cells and Dendritic Cells

This information is current as of March 5, 2022.

Ryutaro Fukui, Atsuo Kanno and Kensuke Miyake

J Immunol 2016; 196:416-427; Prepublished online 30 November 2015;

doi: 10.4049/jimmunol.1500071

<http://www.jimmunol.org/content/196/1/416>

References This article **cites 54 articles**, 23 of which you can access for free at:
<http://www.jimmunol.org/content/196/1/416.full#ref-list-1>

Why *The JI*? Submit online.

- **Rapid Reviews! 30 days*** from submission to initial decision
- **No Triage!** Every submission reviewed by practicing scientists
- **Fast Publication!** 4 weeks from acceptance to publication

**average*

Subscription Information about subscribing to *The Journal of Immunology* is online at:
<http://jimmunol.org/subscription>

Permissions Submit copyright permission requests at:
<http://www.aai.org/About/Publications/JI/copyright.html>

Email Alerts Receive free email-alerts when new articles cite this article. Sign up at:
<http://jimmunol.org/alerts>



Type I IFN Contributes to the Phenotype of *Unc93b1*^{D34A/D34A} Mice by Regulating TLR7 Expression in B Cells and Dendritic Cells

Ryutaro Fukui,* Atsuo Kanno,*[†] and Kensuke Miyake*[†]

TLR7 recognizes pathogen-derived and self-derived RNA, and thus a regulatory system for control of the TLR7 response is required to avoid excessive activation. Unc93 homolog B1 (Unc93B1) is a regulator of TLR7 that controls the TLR7 response by transporting TLR7 from the endoplasmic reticulum to endolysosomes. We have previously shown that a D34A mutation in Unc93B1 induces hyperactivation of TLR7, and that *Unc93b1*^{D34A/D34A} mice (D34A mice) have systemic inflammation spontaneously. In this study, we examined the roles of inflammatory cytokines such as IFN- γ , IL-17A, and type I IFNs to understand the mechanism underlying the phenotype in D34A mice. mRNAs for IFN- γ and IL-17A in CD4⁺ T cells increased, but inflammatory phenotype manifesting as thrombocytopenia and splenomegaly was still observed in *Ifng*^{-/-} or *Il17a*^{-/-} D34A mice. In contrast to T cell-derived cytokines, *Ifnar1*^{-/-} D34A mice showed an ameliorated phenotype with lower expression of TLR7 in B cells and conventional dendritic cells (cDCs). The amount of TLR7 decreased in B cells from *Ifnar1*^{-/-} D34A mice, but the percentage of TLR7⁺ cells decreased among CD8 α ⁻ cDCs. In conclusion, type I IFNs maintain expression of TLR7 in B cells and cDCs in different ways; total amount of TLR7 is kept in B cells and TLR7⁺ population is retained among cDCs. Our results suggested that these TLR7-expressing cells are activated initially and influence TLR7-dependent systemic inflammation. *The Journal of Immunology*, 2016, 196: 416–427.

Toll-like receptors are a family of innate immune sensors that recognize pathogen-associated molecular patterns (PAMPs) and activate immune responses (1–3). In addition to microbial products, TLRs respond to host-derived molecules and induce noninfectious inflammation (4, 5). Because nucleic acids have conserved structures in the host and microbes, dysregulation of nucleic acid-sensing TLRs leads to inflammatory diseases such as systemic lupus erythematosus (SLE) (6–9). To avoid excessive inflammation, nucleic acid-sensing TLRs need to be strictly regulated (10).

We previously showed that Unc93 homolog B1 (Unc93B1) plays a role in preventing hyperactivation of TLR7, a sensor for ssRNA (11). Unc93B1 is a multimembrane-spanning protein that binds to nucleic acid-sensing TLRs on the endoplasmic reticulum membrane and transports them from endoplasmic reticulum to endolysosomes (12, 13). Nucleic acid-sensing TLRs recognize their ligands in endolysosomes (14); therefore, Unc93B1 is an essential regulator of nucleic acid-sensing TLRs (15). We found that Unc93B1 also controls the responses of TLRs depending on its N-terminal region and that a D34A mutation in Unc93B1 enhances the TLR7 response and attenuates the TLR9 response (11). Mice harboring the D34A mutation (*Unc93b1*^{D34A/D34A} mice, D34A mice) have systemic lethal inflammation due to TLR7 hyperactivation, with resultant thrombocytopenia, splenomegaly, hepatitis, and premature death (16). Unc93B1 is thought to be important for maintaining homeostasis, and thus we focused on activated cells and cytokines for a deeper analysis of the phenotype in D34A mice.

In D34A mice, CD4⁺ T cells are spontaneously activated and differentiated into Th1 and Th17 subsets by TLR7 hyperactivation (16). These subsets produce IFN- γ or IL-17A, respectively, and induce various types of autoimmune diseases (17). It is thought that role for TLRs in the activation of T cells is not cell autonomous, but relation between TLRs and activation of these T cells are reported as a factor of inflammation (18–20). Not only T cells, B cells are also activated in D34A mice and play important roles. Because TLR7 expression in B cells is dependent on type I IFNs (21, 22), type I IFNs may have a role in systemic lethal inflammation.

In this study, to examine the roles of T cell-derived cytokines and type I IFNs, D34A mice were crossed with mice lacking T cell-derived cytokines or the receptor for type I IFNs. Interestingly, the lack of type I IFN signaling was more effective than that of IFN- γ or IL-17A for ameliorating systemic inflammation in D34A mice. This may be because the lack of type I IFN signaling appreciably downregulated TLR7 expression in B cells

*Division of Innate Immunity, Department of Microbiology and Immunology, The Institute of Medical Science, The University of Tokyo, Tokyo 108-8639, Japan; and [†]Laboratory of Innate Immunity, Center for Experimental Medicine and Systems Biology, The Institute of Medical Science, The University of Tokyo, Tokyo 108-8639, Japan
Received for publication January 12, 2015. Accepted for publication October 30, 2015.

This work was supported by Japan Society for the Promotion of Science Grants-in-Aid for Scientific Research A and C, 25253032 and 25460585, Grant-in-Aid for Exploratory Research 26670235, Ministry of Education, Culture, Sports, Science and Technology Grant-in-Aid for Scientific Research on Innovative Areas 21117002, the Translational Research Network Program (B), the Mochida Memorial Foundation for Medical and Pharmaceutical Research, the Astellas Foundation for Research on Metabolic Disorders, the Takeda Science Foundation, the SENSHIN Medical Research Foundation, and the Japan Prize Foundation.

R.F. performed the experiments; A.K. developed the anti-TLR7 Ab; R.F., A.K., and K.M. analyzed the results; R.F. made figures; and R.F. and K.M. designed the research and wrote the paper.

Address correspondence and reprint requests to Dr. Kensuke Miyake, Division of Innate Immunity, Department of Microbiology and Immunology, The Institute of Medical Science, The University of Tokyo, 4-6-1 Shirokanedai, Minato-ku, Tokyo 108-8639, Japan. E-mail address: kmiyake@ims.u-tokyo.ac.jp

Abbreviations used in this article: cDC, conventional DC; CD62L, L-selectin; D34A mice, *Unc93b1*^{D34A/D34A} mice; D34A-TCRDKO mouse, *Terb*^{-/-}*Tcrd*^{-/-} D34A mouse; DC, dendritic cell; FoB, follicular B; MZB, marginal zone B; PAMP, pathogen-associated molecular pattern; pDC, plasmacytoid DC; PDCA1, plasmacytoid DC Ag 1; Unc93B1, Unc93 homolog B1; WT, wild-type.

Copyright © 2015 by The American Association of Immunologists, Inc. 0022-1767/15/\$30.00

and also in conventional dendritic cells (cDCs). These results demonstrate an important role of type I IFNs in TLR7-dependent inflammation.

Materials and Methods

Mice

Wild-type (WT) C57BL/6N slc mice were purchased from Japan SLC (Hamamatsu, Japan). *Unc93b1*^{D34A/D34A} mutant mice were generated as described previously (16). The mice were backcrossed to C57BL/6N slc strain at least 12 times. *Ifng*^{-/-} mice and *Il17a*^{-/-} mice were obtained from Dr. Y. Iwakura (Tokyo University of Science, Tokyo, Japan). *Tcrb*^{-/-} *Tcrd*^{-/-} double-knockout mice, and *Ighm*^{-/-} mice were purchased from The Jackson Laboratory. *Ifnar1*^{-/-} mice were purchased from B&K Universal. Mice for the data were sex matched (female) and age matched (indicated in figure legends). These mice were kept in specific pathogen-free condition and used for experiments with the guideline of the University of Tokyo.

Reagents and Abs

Staining buffer was prepared with 1× PBS, 2% FBS, 0.04% NaHCO₃, 2 mM EDTA, and 0.1% NaN₃. For saponin buffer, 0.1% saponin (Sigma-Aldrich, St. Louis, MO) was added in staining buffer. Culture medium for B cells and cDCs was prepared with RPMI 1640 medium (Life Technologies, Waltham, MA), 10% FBS, penicillin–streptomycin/L-Glutamine (Life Technologies), and 50 μM 2-ME. Loxoribine was purchased from Enzo Life Sciences (Farmingdale, NY). Anti-CD16/32, anti-CD19, anti-CD23, anti-CD3e, anti-CD4, anti-CD8α, anti-CD11c, anti-L-selectin (CD62L), anti-Ly6G, anti-plasmacytoid DC Ag 1 (PDCA1),

anti-SiglecH, and mouse IgG1 isotype control Ab were purchased from BioLegend (San Diego, CA). Anti-CD21, anti-CD11b, anti-NK1.1, anti-CD44, and anti-Ly6C were purchased from BD Biosciences. Anti-CD16/32, anti-CD11b and anti-CD8α were also purchased from eBioscience (San Diego, CA, USA). Anti-TLR7 was generated as described in the previous report (23).

Histological analysis

Organs were fixed by 3.7% formaldehyde in PBS and embedded in paraffin wax for section. Sliced organs were stained by H&E. Stained organs were observed by BX41 microscopy (Olympus, Tokyo, Japan) or EVOS FL Auto (Life Technologies).

Cell surface staining

Spleens were obtained from mice and prepared into single-cell suspension. RBCs were lysed by RBC lysis buffer (BioLegend), and left cells were incubated with anti-CD16/32 for blocking FcR. The cells were stained with the following sets of Abs: B cells, anti-CD19, anti-CD21, and anti-CD23; T cells, anti-CD3e, anti-CD4, anti-CD8α, anti-CD44, and anti-CD62L; and myeloid cells or NK cells, anti-CD11b, anti-CD11c, anti-NK1.1, anti-Ly6C, anti-Ly6G, anti-PDCA1, anti-CD4, and anti-CD8α. Stained cells were subjected to further internal staining, FACS analysis, or cell sorting.

Intracellular staining

After cell surface staining, cells were fixed by 4% paraformaldehyde (Thermo Scientific, Waltham, MA) at room temperature for 20 min. Fixed cells were stained with anti-TLR7 or IgG1 isotype control Ab (biotin-conjugated) by incubating in 0.1% saponin buffer at 4°C for 40 min.

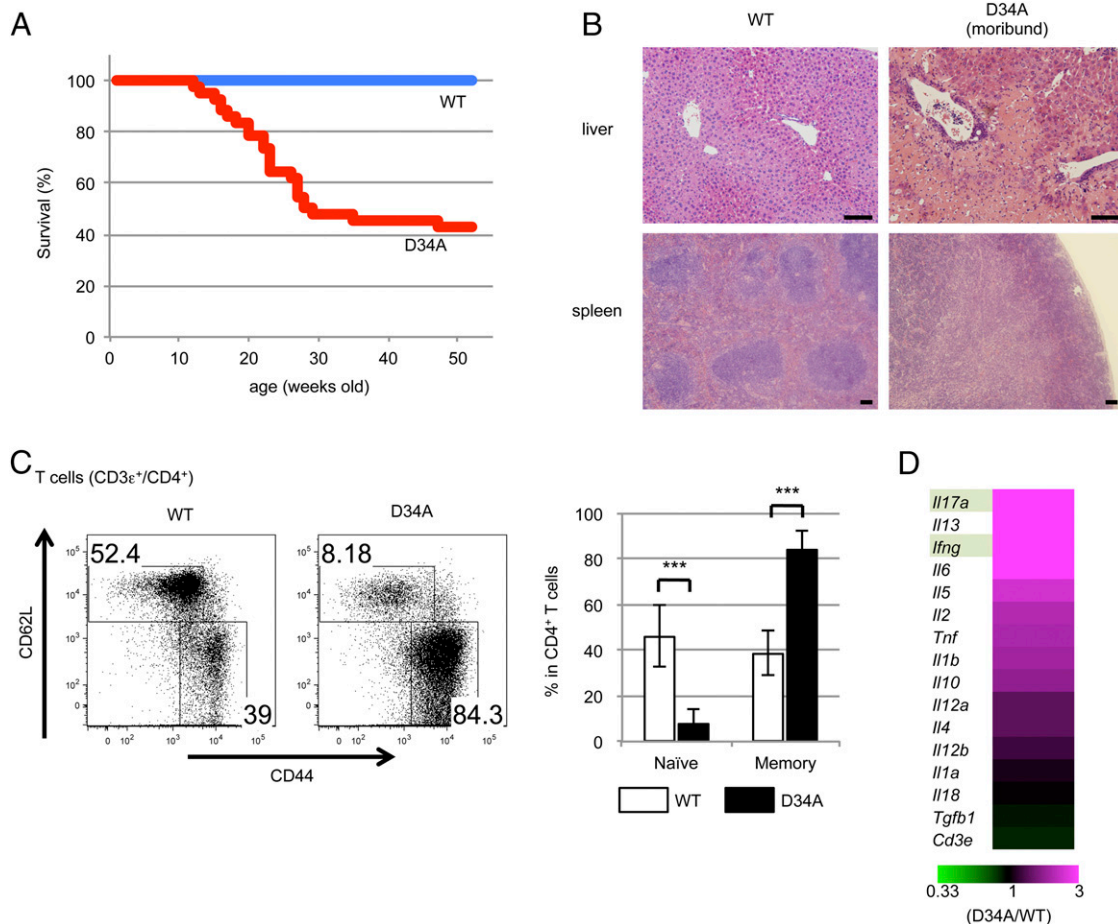


FIGURE 1. Inflammatory phenotypes and T cell activation are observed in C57BL/6 background D34A mice. **(A)** Survival curves of WT ($n = 18$) and D34A ($n = 42$) mice. **(B)** Histological analysis of liver and spleen from WT or moribund D34A mice. Sections of the organs were stained by H&E. **(C)** FACS analysis for CD3e⁺CD4⁺ T cells. CD62L⁺CD44⁻ cells are naive cells and CD62L⁻CD44⁺ cells are memory cells. Representative data are shown by dot plot with frequencies of the cells, and average of the frequencies is shown by graph. **(D)** mRNA of indicated genes were detected by real-time PCR array system, and the ratio of expression level D34A/WT is shown. At least four mice (B–D) sex and age matched were used. Scale bars, 100 μm. *** $p < 0.001$.

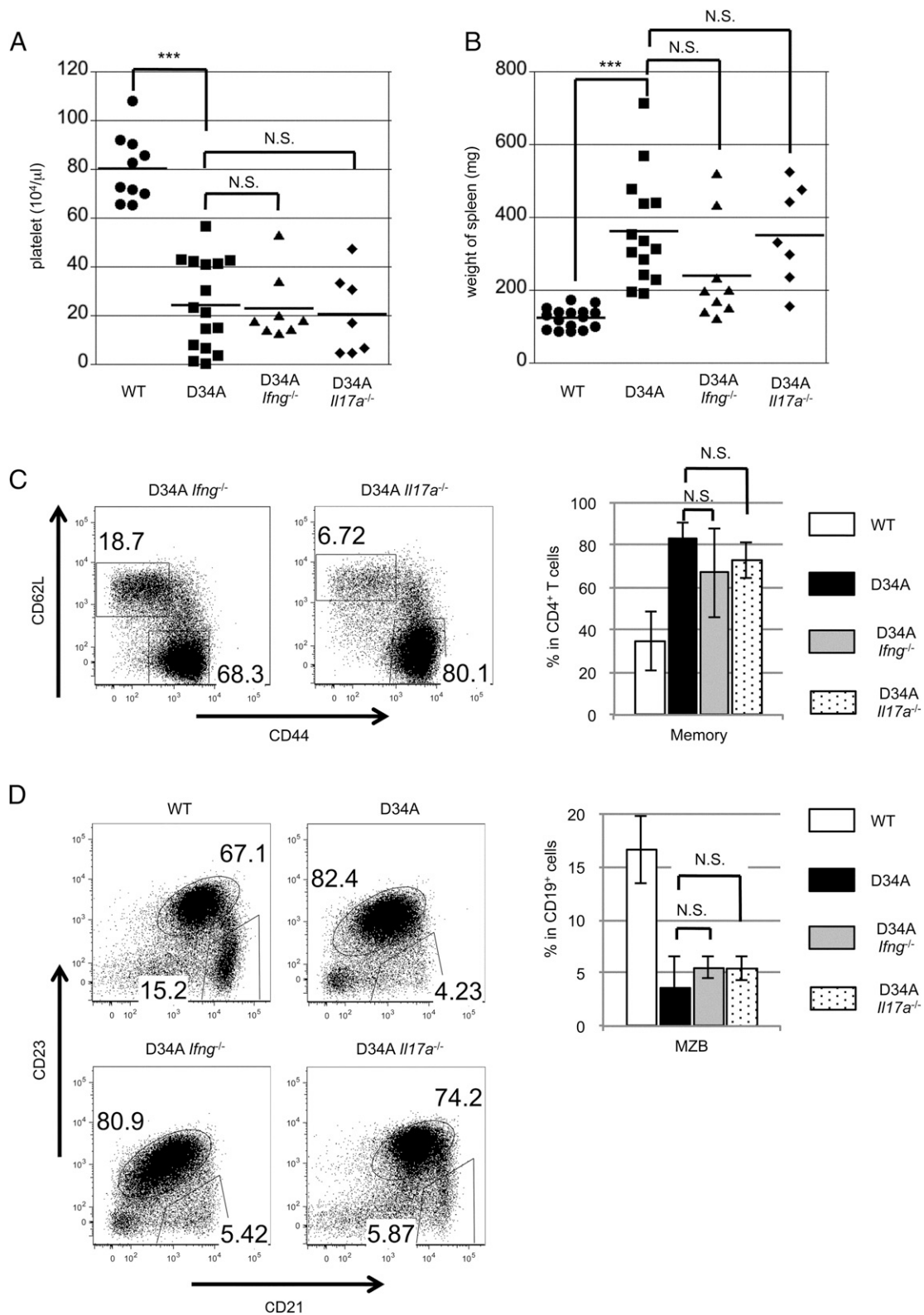


FIGURE 2. Single deletion of IFN- γ or IL-17A in D34A mice does not rescue from inflammatory phenotypes. **(A)** Concentration of platelets in peripheral blood from 4-mo-old mice. **(B)** Weight of spleen from 5- to 7-mo-old mice. **(C)** FACS analysis for CD3e⁺CD4⁺ T cells. **(D)** FACS analysis for CD19⁺ B cells. CD23⁺CD21⁺ cells are FoB cells and CD23⁻CD21⁺ cells are MZB cells. At least seven mice (A and B) or three mice (C and D) sex and age matched were used. Representative data are shown by dot plot with frequencies of the cells, and the average of the frequencies is shown by graph (C and D). Bars in the dot graphs indicate average of the score. ****p* < 0.001.

The cells were washed with staining buffer and stained with streptavidin-PE by incubating in 0.1% saponin buffer at 4°C for 40 min. Stained cells were subjected to FACS analysis.

FACS analysis and cell sorting

Stained cells were analyzed by FACSaria with FACSDiva software (BD, Franklin Lakes, NJ). FACSaria was used also for cells sorting. Obtained data were imported to FlowJo software (FlowJo, Ashland, OR) and analyzed, according to published data (24–26). Gating strategy of FACS was shown in Figs. 8A and 9A.

Cytokine array with real-time PCR

Single-cell suspension of splenocytes was prepared and RBCs were lysed as described above. Cells were stained by anti-CD3e, anti-CD4 and anti-CD8 α , and T cells (CD3e⁺ CD4⁺) were collected by FACSaria. Collected cells were prepared for their RNA with RNeasy kit (QIAGEN, Venlo, the Netherlands). cDNA was synthesized from extracted RNA by ReverTra Ace Quantitative PCR RT Kit (Toyobo, Osaka, Japan). cDNA was mixed with FastStart Universal Probe Master (ROX) (Roche, Basel, Switzerland) and applied to the wells of TaqMan Array Mouse Immune Response (Applied Biosystems, Carlsbad, CA). Expression of the genes were measured by StepOne plus (Life Technologies, Carlsbad, CA) and analyzed by $\Delta\Delta C_t$ protocol. To calculate relative expression of target gene, *Gapdh*, *Actb*, and

Hprt1 were used as internal reference gene, and the average of the quotient was used for data.

Hematological analysis

Whole peripheral blood samples were obtained from tails of mice with EDTA-treated vacuum capillaries (Drummond, Broomall, PA). Hematological scores were measured by automatic hemocytometer MEK-6450 Celltac α (Nihon Kohden, Tokyo, Japan).

B cell proliferation assay

Single-cell suspension of splenocytes was prepared and RBCs were lysed as described above. Cells were treated with B cell isolation kit (Miltenyi Biotec, Bergisch Gladbach, Germany) and subjected to AutoMACS (Miltenyi Biotec). Negative fraction was collected as B cells and suspended in 0.1% BSA-PBS (2×10^6 cells/ml). Cell trace CFSE Cell Proliferation Kit (Life Technologies) was added in the suspension and mix well (final concentration: 2 μ M). Cells were incubated in 37°C for 10 min, and ice-cold culture medium (same volume to suspension) was added. It was incubated on ice for 5 min and centrifuged. Cell pellet was suspended in fresh ice-cold culture medium and centrifuged for wash. After three times of wash, cells were suspended in fresh culture medium and seeded on 96-well round bottom plate. Cells were stimulated by ligands and incubated in 37°C for 3 d. Proliferation of cells was detected

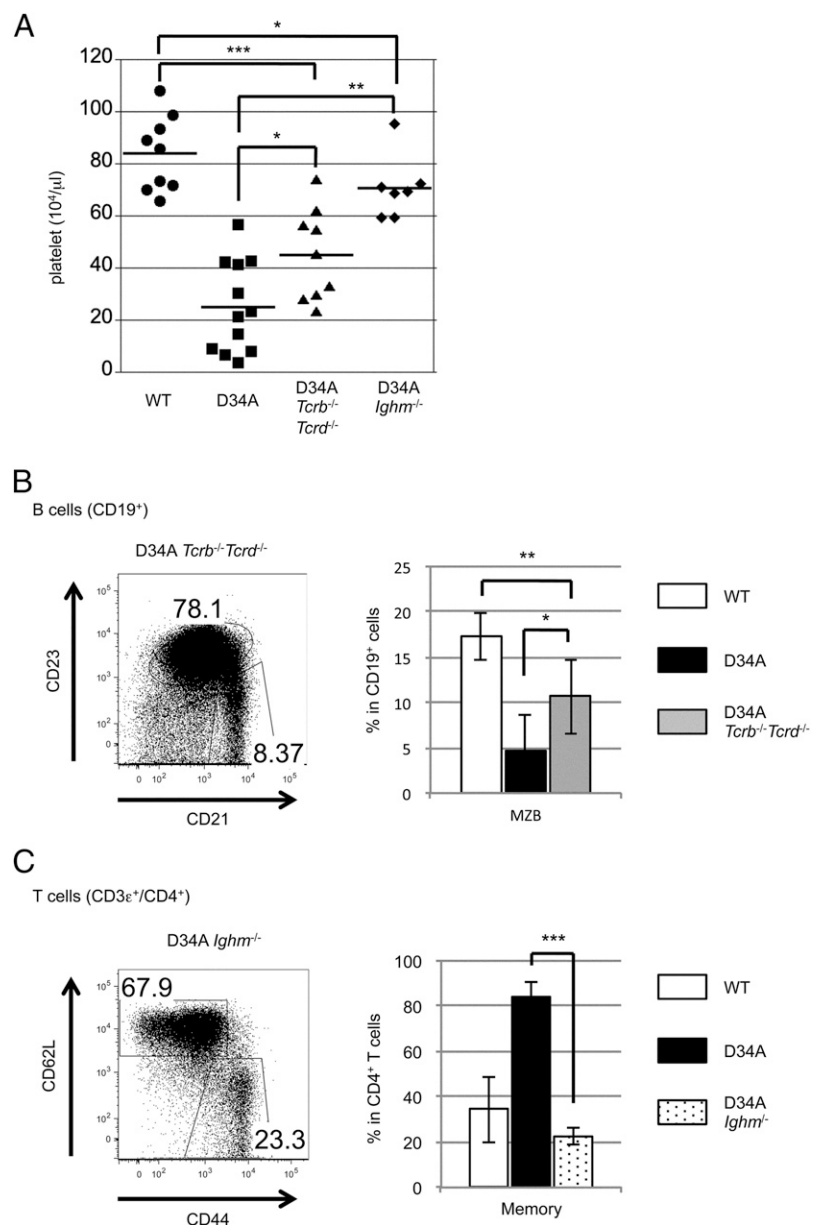


FIGURE 3. B cells have priority of activation over T cells in D34A mice. **(A)** Concentration of platelets in peripheral blood from 4-mo-old mice. **(B)** FACS analysis for CD19⁺ B cells. **(C)** FACS analysis for CD3e⁺ CD4⁺ T cells. At least seven mice (A) or three mice (B and C) sex and age matched were used. Bars in the dot graphs indicate average of the score. Representative data are shown by dot plot with frequencies of the cells, and average of the frequencies is shown by graph. **p* < 0.05, ***p* < 0.01, ****p* < 0.001.

as the reduction of CFSE with FACSVerse or FACSCalibur (BD Biosciences).

Stimulation of DCs

Single-cell suspension of splenocytes was prepared and RBCs were lysed as described above. Cells were treated with anti-CD-16/32 for Fc block and subjected to the incubation with *Pan* DC microbeads (Miltenyi Biotec). Positive fraction was collected by AutoMACS and proceeded further staining. Cells were stained by anti-CD11c, anti-SiglecH, anti-CD8 α , and anti-NK1.1. Stained cells were sorted by FACSaria and CD8 α ⁺ cDCs were collected. Collected cells were suspended in culture medium and seeded on 96-well round bottom plate. Cells were stimulated by ligand and supernatant was collected after 24 h for ELISA.

ELISA

IL-6 in culture supernatant was detected by Mouse IL-6 ELISA Ready-SET-Go! (eBioscience). Serum IFN- α or IFN- β was detected by VeriKine Mouse IFN- α ELISA Kit or VeriKine-HS Mouse IFN- β Serum ELISA Kit, respectively (PBL Assay Science, Piscataway, NJ).

Statistical analysis

Student *t* test was performed to compare the data by Kaleida Graph software or Microsoft Excel software. Two-way ANOVA was performed by Kaleida Graph software to compare the data from WT, D34A, *Ifnar1*^{-/-},

and D34A/*Ifnar1*^{-/-} mice. If the *p* value was <0.05, the difference was judged as significant.

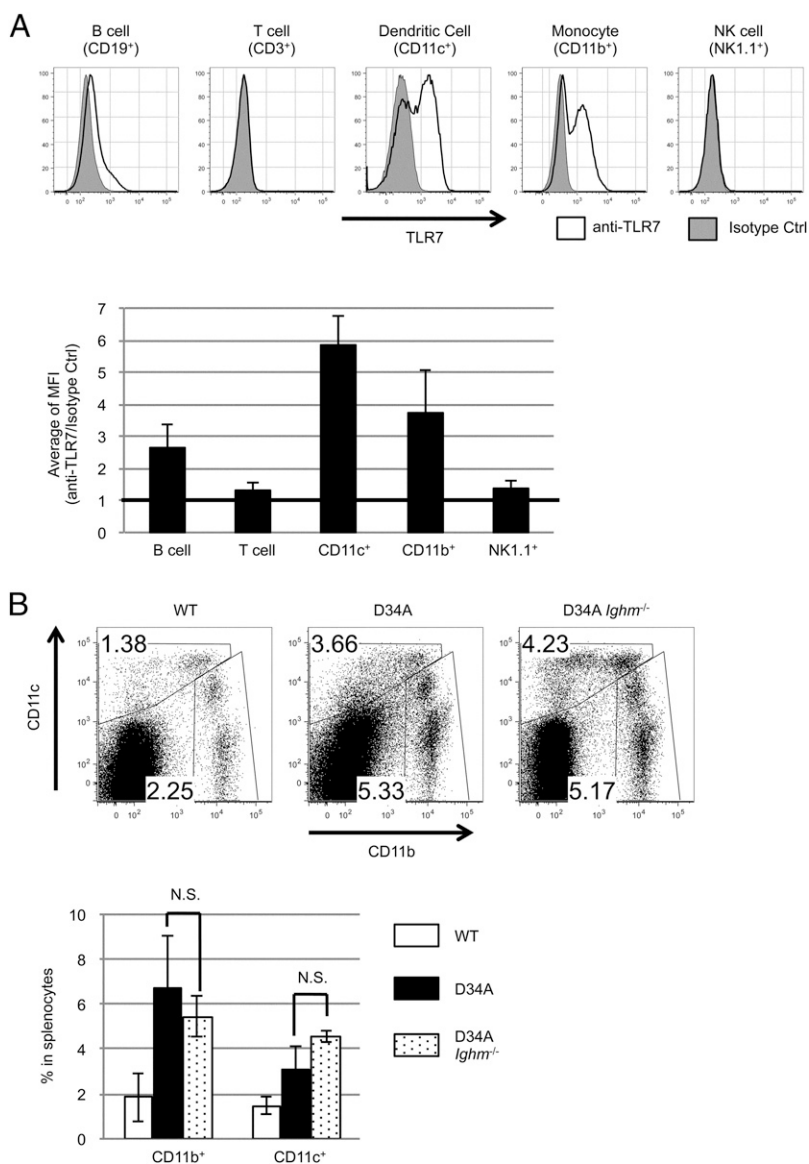
Results

IFN- γ or IL-17A is not a critical factor of the phenotype in D34A mice

We originally developed D34A mice by using 129^{ola} strain based ES cells (16). To cross with other mutant mice, D34A mice were first backcrossed with C57BL/6N mice at least 12 times. The C57BL/6N background did not alter systemic inflammation, which led to premature death, hepatitis, thrombocytopenia, and splenomegaly (Figs. 1A, 1B, 2A, 2B). As reported previously, almost all CD4⁺ T cells were differentiated into memory T cells in D34A mice and expressed a variety of cytokines, including IFN- γ and IL-17A (Fig. 1C, 1D).

To examine the role of IFN- γ and IL-17A in systemic inflammation in D34A mice, we generated *Ifng*^{-/-} or *Il17a*^{-/-} D34A mice. Splenomegaly was slightly reduced by lack of IFN- γ (*p* = 0.064), but no significant changes in thrombocytopenia and splenomegaly. Expansion of memory T cells was observed in these mice with statistic analysis (Fig. 2A–C). Marginal zone B (MZB) cells (CD19⁺CD21⁺CD23⁻, MZB cells) were decreased in D34A mice (Fig. 2D), as in other TLR7-hyperactivated mice such

FIGURE 4. TLR7 expression pattern is correlated to the activation of cells in D34A mice. **(A)** FACS analysis for endogenous TLR7 in cells. Cell surface was stained with indicated lineage markers, and cell interior was stained by anti-TLR7 (clone: A94B10, IgG1) or non-immunized IgG1 isotype control Ab. Ratio of mean fluorescence intensity was calculated and shown by graph. **(B)** FACS analysis for CD11c⁺ DCs or CD11b⁺ monocytes. To avoid including CD11b⁺/CD11c⁺ NK cells, NK1.1⁻ population is shown on the plots. At least four mice (A) or three mice (B) sex and age matched were used. Representative data are shown by histogram (A) or dot plot with the average of frequencies (B).



as Yaa mice (8, 27). Deletion of IFN- γ or IL-17A did not rescue the decrease in MZB cells.

Next, to study the T cell contribution to inflammation in D34A mice, *Tcrb*^{-/-}*Tcrd*^{-/-} D34A mice (D34A-TCRDKO) were generated. In these mice, the platelet count in the circulation was significantly increased but was still lower than those in WT mice and B cell-deficient (*Ighm*^{-/-}) D34A mice (Fig. 3A). Reduction of MZB cells was ameliorated by T cell deficiency but still observed, suggesting that B cells were activated independently of T cells (Fig. 3B).

TLR7-expressing cells are initially activated in D34A mice

Spontaneous T cell activation in D34A mice was not seen in B cell-deficient D34A mice (Fig. 3C), demonstrating that T cell activation is dependent on B cells. B cell-dependent T cell activation is consistent to the previous studies on MRL^{lpr/lpr} mice (28, 29). T cell activation by activated B cells is likely to play a key role in autoimmune models.

Given that TLR7 drives pathogenic inflammation in D34A mice, it is important to study TLR7 expression in a variety of immune

cells. FACS analyses with a recently established anti-mouse TLR7 mAb (23) revealed that B cells, CD11c⁺ cells, and CD11b⁺ cells expressed TLR7, whereas TLR7 was undetectable in T cells and NK cells (Fig. 4A). TLR7-expressing cells are likely to be primarily activated in D34A mice, and B cells are activated in D34A mice (16). Given TLR7 expression, DCs and monocytes are also likely to be activated by TLR7 in D34A mice. As expected, DCs and monocytes expanded in the spleen in D34A mice (Fig. 4B). Interestingly, this expansion was even observed in *Ighm*^{-/-} D34A mice, suggesting that myeloid cells were autonomously activated in D34A mice.

Type I IFNs maintain TLR7 expression in B cells and keep the phenotype in D34A mice

TLR7 expression in B cells is enhanced by type I IFNs (21, 22), and type I IFN plays important role for TLR7-driven autoimmune phenotypes in MRL^{lpr/lpr} mice (9, 30). These reports suggest that type I IFN, TLR7, and B cell are tightly interacting with each other in some autoimmune models. To understand the roles of type I IFNs in inflammation in D34A mice, we generated

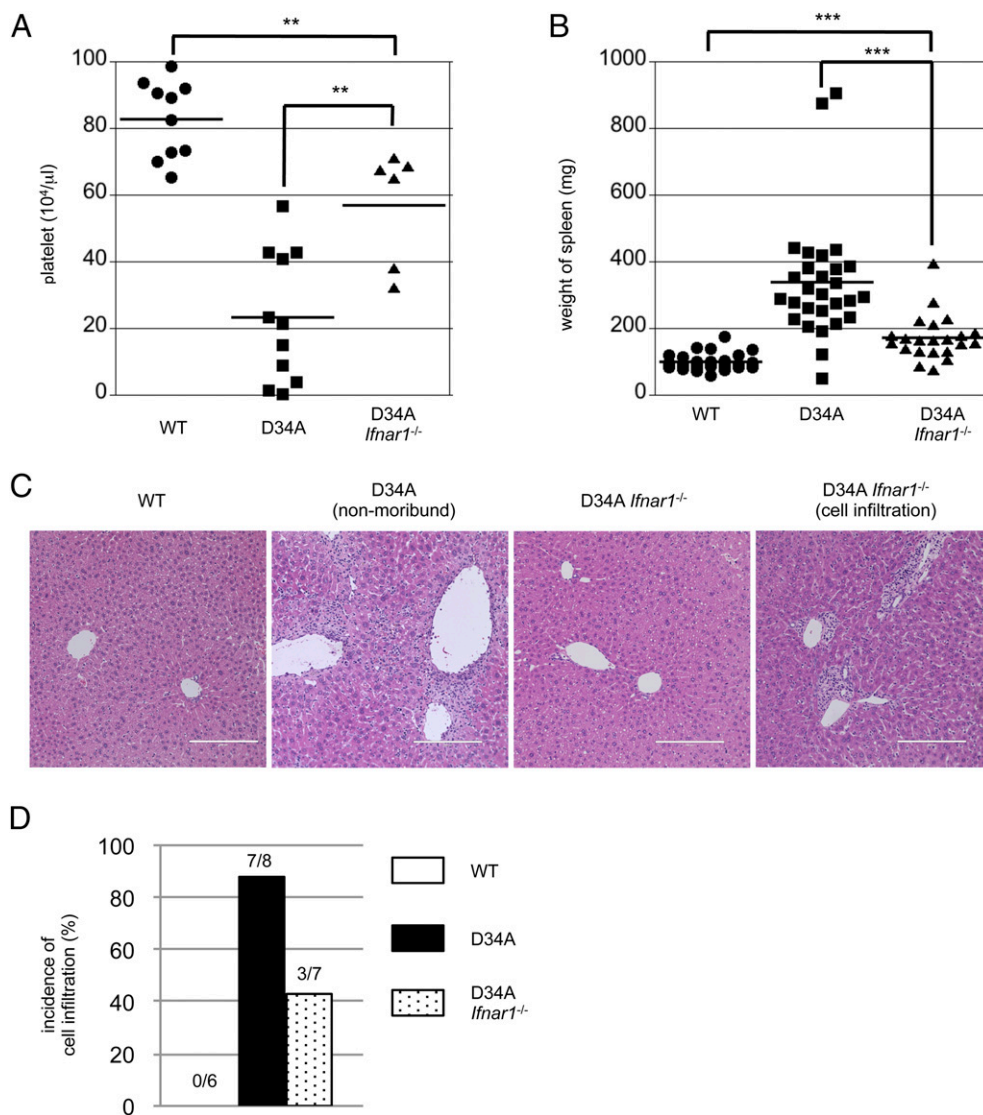


FIGURE 5. Type I IFN signaling contributes to the phenotypes of D34A mice (**A**) Concentration of platelets in peripheral blood from 4-mo-old mice. (**B**) Weight of spleen from 4- to 6-mo-old mice. (**C**) H&E stained histological images of liver. Scale bars, 200 μ m. (**D**) Incidence of cell infiltration in liver. Numbers of the mice, which have indicated phenotype, are shown by graph. At least 6 mice (A), 22 mice (B), or 6 mice (C and D) sex and age matched were used. ** $p < 0.01$, *** $p < 0.001$.

Ifnar1^{-/-} D34A mice. These mice had significant amelioration of thrombocytopenia, splenomegaly, and hepatitis with cell infiltration (Fig. 5). The percentage of MZB cells were increased (Fig. 6A), and in association with the effects on B cells, T cells were also affected and less memory CD4⁺ T cells were found in *Ifnar1*^{-/-} D34A mice (Fig. 6B). Of note, the expansion of splenic CD11b⁺ or CD11c⁺ cells observed in B cell-deficient D34A mice was decreased in *Ifnar1*^{-/-} D34A mice (Fig. 6C).

To study the relationship between type I IFNs and TLR7, expression of TLR7 in B cells was analyzed by flow cytometry. As found previously (21, 22), less TLR7 was expressed in splenic B cells from *Ifnar1*^{-/-} mice (Fig. 7A). D34A mutation in Unc93B1 did not alter the expression of TLR7 in B cells, and the lack of type I IFN signaling in D34A mice reduced the expression of TLR7 (Fig. 7A). Interestingly, TLR7 expression in MZB cells

was much higher than in follicular B (FoB) cells and was even detectable in type I IFN-deficient mice (Fig. 7A). To see the consequence of reduced TLR7 expression in TLR7 responses, TLR7-dependent B cell proliferation was studied. As reported previously, TLR7-dependent B cell proliferation was severely impaired by the lack of type I IFNR (Fig. 7B). D34A mutation failed to enhance the responses of *Ifnar1*^{-/-} B cells. These results are consistent with ameliorated inflammation in *Ifnar1*^{-/-} D34A mice.

Type I IFNs control the population pattern and expression of TLR7 in cDCs

Activation of B cells in D34A mice might be dependent on the amount of TLR7 maintained by type I IFNs. Unexpectedly, expansion of splenic CD11b⁺ cells and CD11c⁺ cells was reduced in *Ifnar1*^{-/-} D34A mice but not in *Ighm*^{-/-} D34A mice (Fig. 4B),

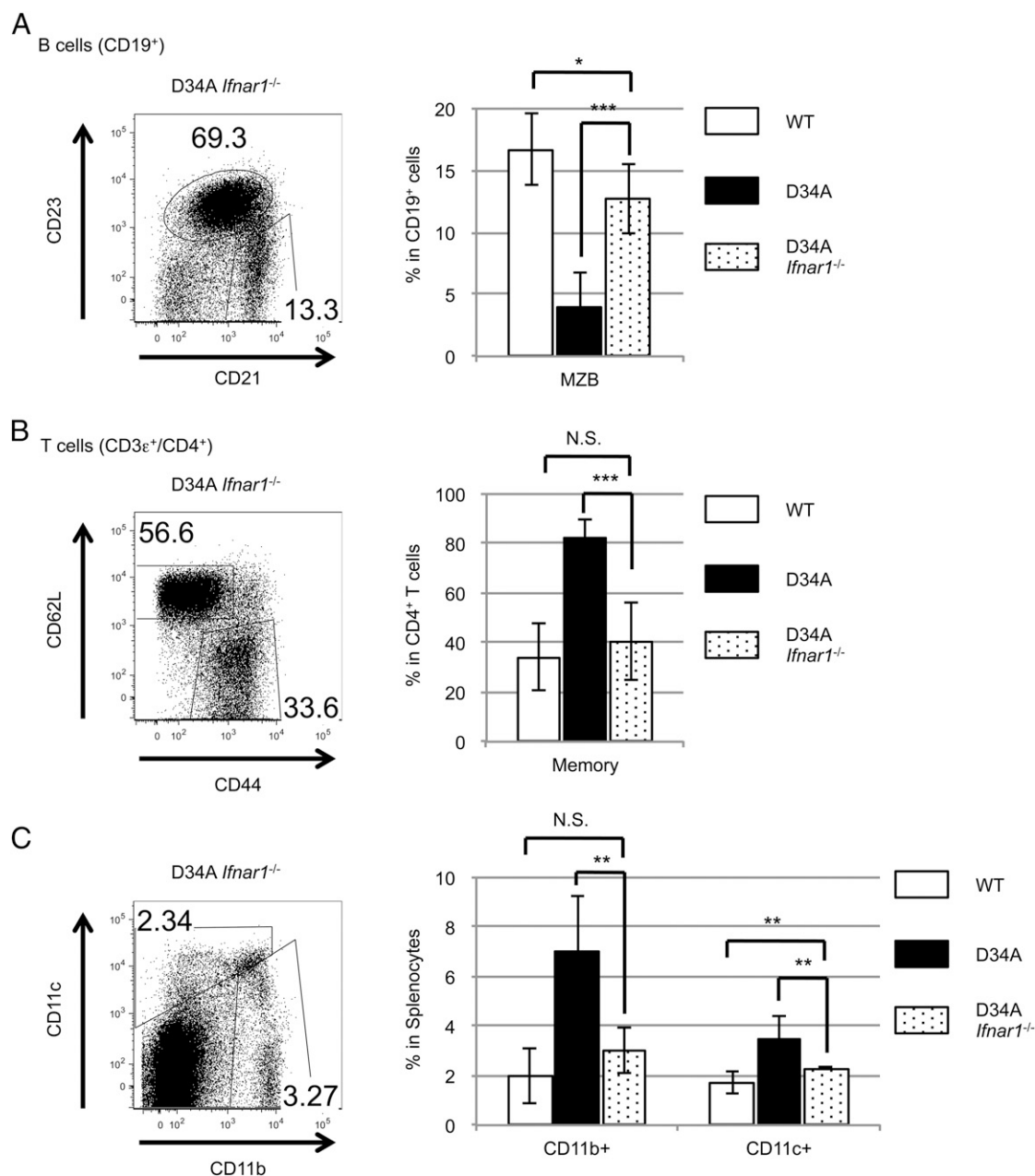


FIGURE 6. Abnormal cell activation in D34A mice is attenuated by the lack of type I IFN signaling. FACS analysis for CD19⁺ B cells (**A**), CD3ε⁺CD4⁺ T cells (**B**), and myeloid cells (**C**). At least six mice sex and age matched were used. Representative data are shown by dot plot with frequencies of the cells, and the average of the frequencies is shown by graph. **p* < 0.05, ***p* < 0.01, ****p* < 0.001.

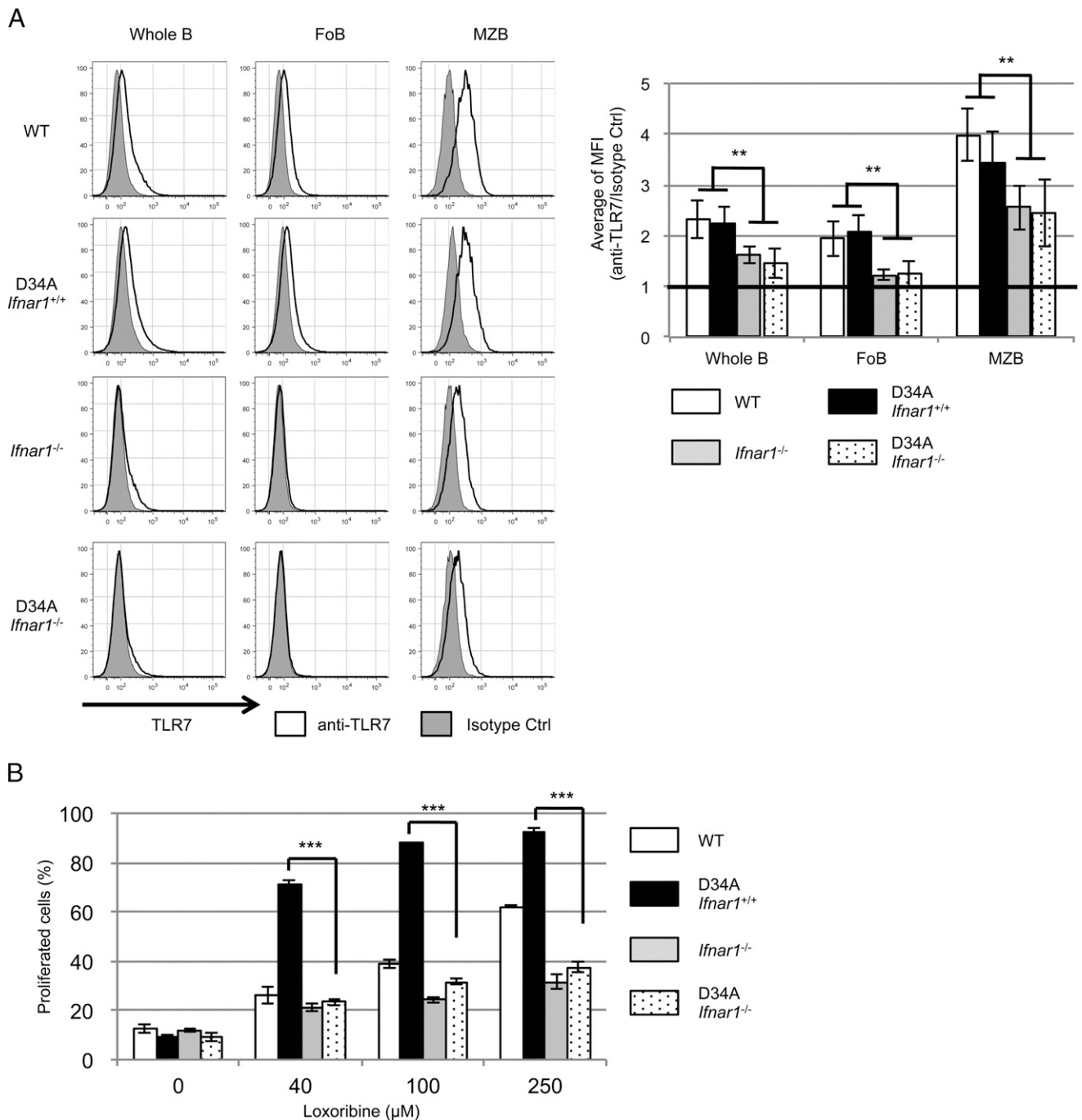


FIGURE 7. Endogenous TLR7 expression in B cells is maintained by type I IFNs. **(A)** FACS analysis for CD19⁺ B cells. Cell surface was stained with anti-CD21 and anti-CD23 to gate FoB cells or MZB cells. Intracellular endogenous TLR7 was also stained as shown in Fig. 4. The ratio of mean fluorescence intensity was calculated and shown by graph. Representative data are shown by histogram. **(B)** Proliferation of B cells after stimulation with TLR7 ligand. Proliferated cells are detected by CFSE labeling assay, and the percentage in total cells is shown by graph. At least three mice sex and age matched were used (A and B). B cells were stimulated in triplicated wells and the mean SD is shown (B). ***p* < 0.01, ****p* < 0.001.

raising the possibility that type I IFNs control expression of TLR7 not only in B cells but also in myeloid cells. To address this possibility, we performed a detailed analysis of TLR7 expression in myeloid cells.

First, we analyzed splenic CD11b⁺ cells, and found that expression of TLR7 in neutrophils (Ly-6G⁺), inflammatory monocytes (Ly-6G⁻, Ly-6C⁺), and macrophages (Ly-6G⁻, Ly-6C⁻) was not affected by IFNAR1 deficiency (Fig. 8A, 8B). Next, we stained TLR7 in splenic pDCs and cDC subsets (31, 32). The

TLR7 expression level was not altered in *Ifnar1*^{-/-} pDCs (CD11c⁺, PDCA11⁺) (Fig. 9A, 9B). In cDCs (CD11c^{hi}, PDCA1) TLR7 was mainly expressed in a CD8α⁻ subset and the TLR7⁺ population was increased in *Ifnar1*^{-/-} mice (Fig. 9B). These results suggest that type I IFNs affect TLR7 expression in CD8α⁻ cDCs.

Finally, we focused on the expression pattern of TLR7 in CD8α⁻ cDCs and compared the populations among WT, D34A, *Ifnar1*^{-/-}, or *Ifnar1*^{-/-} D34A mice. The main population of TLR7-expressing

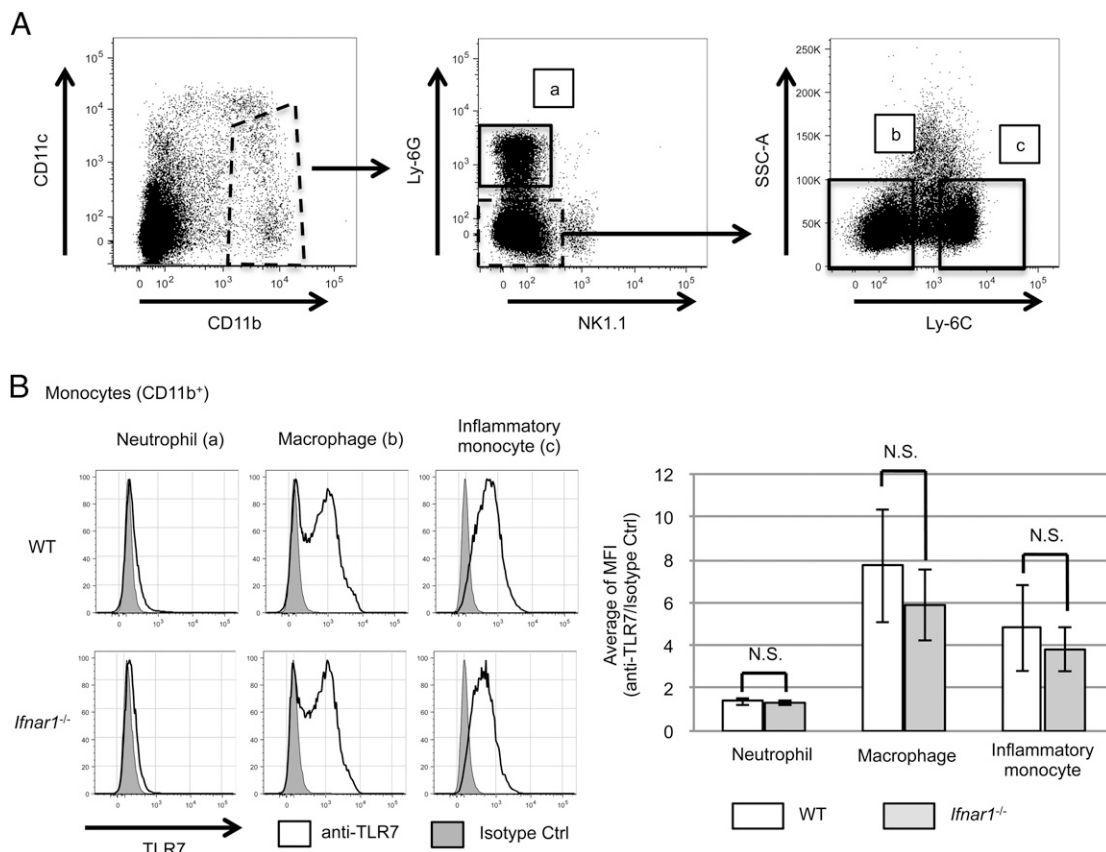


FIGURE 8. TLR7 expression in monocytes is not altered by the deficiency of type I IFNs. FACS analysis for CD11b⁺ monocytes. Cell surface was stained with anti-CD11b, anti-CD11c, anti-NK1.1, anti-Ly6C, and anti-Ly6G to gate neutrophils, inflammatory monocytes, and macrophages. **(A)** Gating strategy for analysis of monocytes. To avoid CD11b⁺ NK cells, NK1.1⁺ cells were gated out first. Cells in the dotted gates were subjected to drill-down analysis. Populations a, b, and c were considered as neutrophils, macrophages, and inflammatory monocytes, respectively. **(B)** TLR7 expression in monocytes. The ratio of mean fluorescence intensity was calculated and shown by graph. Representative data are shown by histogram. At least three mice sex and age matched were used.

cells was CD4⁺ in WT mice, whereas CD4⁻CD8⁺ (double-negative [DN]) in D34A mice (Fig. 10A). IFNAR1 deficiency decreased the TLR7-expressing population, especially TLR7⁺ DN cDCs (Fig. 10A, compare right lower quadrants between D34A and *Ifnar1*^{-/-} mice). Because of this effect, TLR7-expressing cells were decreased in *Ifnar1*^{-/-} D34A mice (Fig. 10A). To see the effect of this population change on TLR7 responses, we purified CD8⁺ cDCs and stimulate them with TLR7 ligand. cDCs from *Ifnar1*^{-/-} or *Ifnar1*^{-/-} D34A mice showed significantly lower IL-6 production than WT or D34A mice, respectively (Fig. 10B). These results demonstrate that type I IFNs homeostatically induce TLR7 expression in cDCs and maintains expansion of TLR7⁺ cells under TLR7-dependent inflammatory conditions.

Discussion

The roles of several cytokines in TLR7-dependent systemic inflammation in D34A mice were addressed in this study, and type I IFN-dependent TLR7 expression in B cells and cDCs was found to have an important role in the systemic inflammation of D34A mice. Although a variety of cells are activated in D34A mice, it is important to determine the cell type primarily responsible for inflammation. According to the results from T cell- or B cell-deficient D34A mice, B cells and myeloid cells were initially activated in D34A mice. In contrast, T cell activation was dependent on B cells.

Both of Th1 and Th17 expanded in D34A mice in a manner dependent on TLR7 (16). To ask whether T cell-derived cyto-

kines such as IFN- γ and IL-17A contribute to the phenotypes in D34A mice, D34A mice were crossed with mice lacking IL-17A or IFN- γ in this study. The lack of neither IL-17A nor IFN- γ ameliorated thrombocytopenia, splenomegaly, and B cell activation. In contrast, the lack of T cells ameliorated thrombocytopenia and the activation of B cells. These data suggest that T cell-derived cytokines other than IL-17A or IFN- γ are responsible for the inflammation in D34A mice. Alternatively, IL-17A and IFN- γ may play redundant roles with each other in D34A mice. Considering that the deletion of IFN- γ reduced splenomegaly to a certain degree ($p = 0.064$), deletions of both IFN- γ and IL-17A might rescue the phenotype in D34A mice.

Systemic inflammation in D34A mice was ameliorated by the lack of IFNAR1 because of downregulated expression of TLR7 in B cells and cDCs. We previously confirmed that the expression of mRNA for TLR7 is not changed by D34A mutation of Unc93B1 in bone marrow-derived DCs, macrophages, and splenic whole B cells (16). In this study, we showed that the expression of TLR7 protein was not altered in B cells but increased in splenic cDCs because of the increase in percentage of TLR7⁺CD8⁺ cDCs. The lack of type I IFN signaling decreased CD8⁺CD4⁻TLR7⁺ cDCs but increased CD8⁺CD4⁺TLR7⁻ cDCs. CD8⁺CD4⁻TLR7⁺ cDC subset drastically increased in percentage in D34A mice, thus CD8⁺CD4⁻TLR7⁺ cDCs are likely to expand in a manner dependent on both TLR7 and type I IFNs.

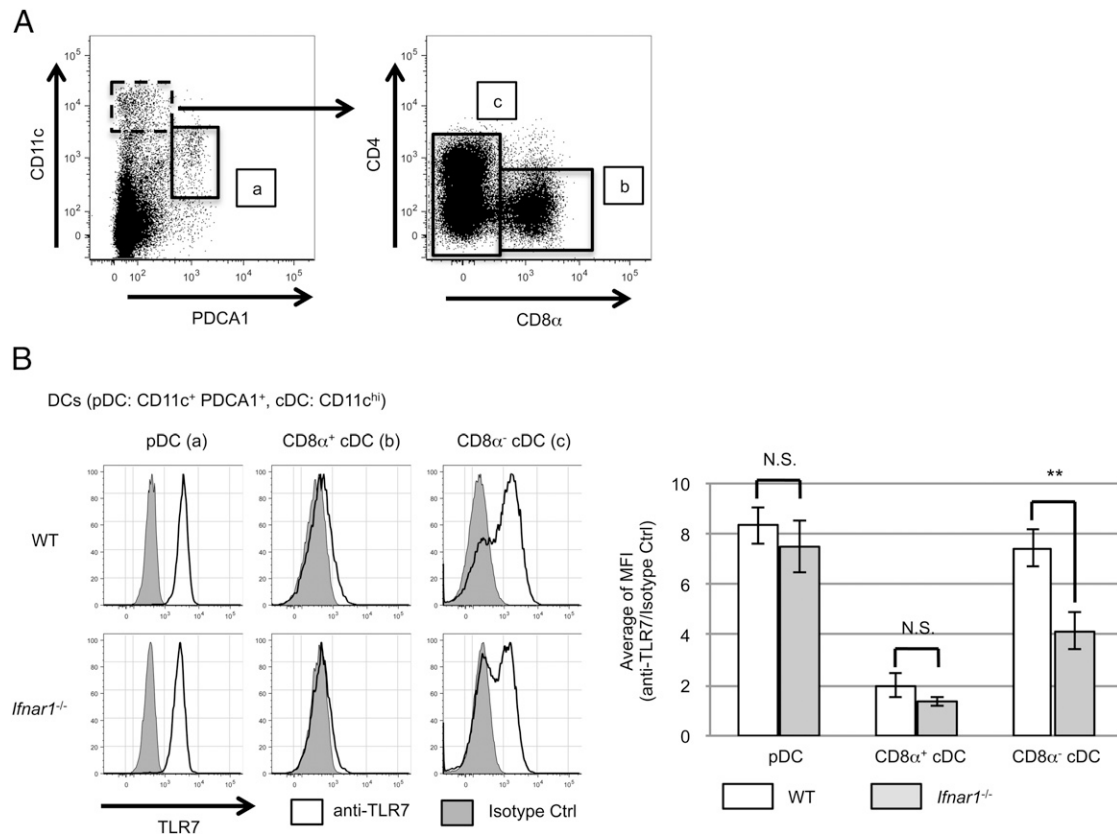


FIGURE 9. Population pattern of TLR7-expressing cDC is controlled by type I IFNs FACS analysis for CD11c⁺ DCs. Cell surface was stained with anti-CD11c, anti-NK1.1, anti-PDCA1, and anti-CD8α to gate pDCs and cDCs. **(A)** Gating strategy for analysis of DCs. To avoid CD11c⁺ NK cells, NK1.1⁺ cells were gated out first. Cells in the dotted gate were subjected to drill-down analysis. Populations a, b, and c were considered as pDCs, CD8α⁺ cDCs, and CD8α⁻ cDCs. **(B)** TLR7 expression in pDCs and cDCs. The ratio of mean fluorescence intensity was calculated and shown by graph. Representative data are shown by histogram. At least four mice sex and age matched were used. ***p* < 0.01.

Previous reports show the functional difference between CD4⁺ and CD4⁻ CD8α⁻ cDCs (33, 34). CD8α⁻ cDCs activate CD4⁺ or CD8α⁺ T cells, but the ability is not dependent on CD4⁺ expression on cDCs (35). In contrast, CD4⁻ cDCs activate iNKT cells more effectively than CD4⁺ cDCs (35). iNKT cells are localized in the marginal zone and known to activate splenic B cells (36, 37). MZB cells also activate iNKT cells (38). NKT cells are also shown to regulate the activation of autoreactive B cells (39, 40). NKT cells seem to specifically suppress autoreactive B cells by a CD1d-dependent manner. The interaction among CD4⁻ CD8α⁻ cDCs, iNKT cell, and B cells is likely to have a key role in the phenotypes of D34A mice.

Aberrant expansion of CD11b⁺ monocytes in D34A mice was abolished by the lack of type I IFN signaling. Considering that TLR7 expression in CD11b⁺ monocytes was not altered by the lack of type I IFN signaling, type I IFN contributes to their expansion not by increasing TLR7 expression. Type I IFN may directly induce monocyte expansion with basal expression of TLR7 or indirectly through the expansion of CD8α⁻ CD4⁻ TLR7⁺ cDCs.

The results in this study suggest that the type I IFN signaling pathway is a promising target for therapeutic intervention in TLR7-dependent inflammatory diseases. It is already known that type I IFN positively regulates TLR7 responses in B cells in autoimmune diseases (41). For example, SLE patients have increased level of IFN-α in serum and autoantibodies (42–44), and TLR7 is shown to drive autoantibody production in murine models (7, 9). Type I IFNs enhance transcription of IFN-related genes, and the elevated

expression of these genes is found in SLE patients as a type I IFN signature (45, 46). Expression of TLR7 is a signature of type I IFN, and TLR7 hyperactivation might be blocked by therapeutic intervention in type I IFN signaling.

Although contribution of type I IFN signaling to the phenotypes of D34A mice is apparent, production of type I IFN is not enhanced like other autoimmune mice. Serum IFN-α is increased in MRL^{lpr/lpr} and New Zealand Black mice, and type I IFN signaling plays key role in autoimmune responses in these mice (9, 30, 47–50). In D34A mice, concentration of serum IFN-α or IFN-β was not detectable by ELISA (data not shown). The serum level of ANA in D34A mice is lower than that in MRL^{lpr/lpr} mice (16). This may be explained by the lack of overproduction of type I IFN. The role of type I IFN in the pathology of D34A mice is to control TLR7 expression in B cells and cDCs.

Our data imply that IFNAR1 on B cells and cDCs is an effective target to reduce TLR7-dependent inflammation. Considering that type I IFNs have protective roles in infectious disease (51, 52), global inhibition of type I IFN signaling is likely to cause adverse effects such as viral infection. By using bispecific Abs against IFNAR1 and the specific surface marker for B cells and cDCs, the expression of TLR7 and activation of these cells are selectively attenuated. There are various subtypes of type I IFNs whereas the heterodimer of IFNAR1 and IFNAR2 works as their common receptor (53, 54); therefore, IFNAR1 is better than type I IFNs as a target. It is important to analyze conditional deletion of *Ifnar1* gene to confirm the specificity as further investigation.

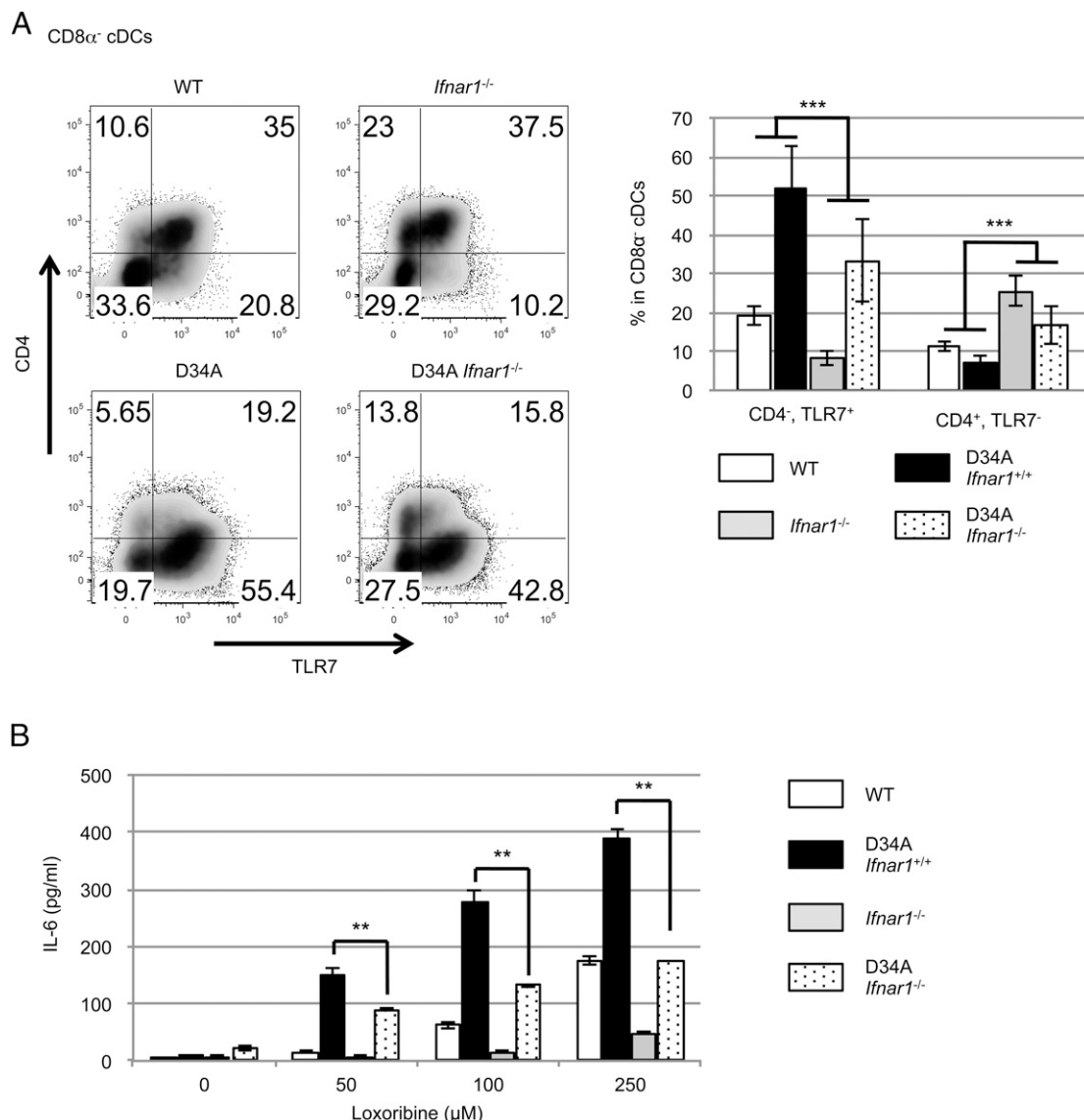


FIGURE 10. Type I IFN signaling maintain TLR7-expressing CD8 α ⁺ cDCs and keep their response against TLR7 ligand. **(A)** FACS analysis for CD8 α ⁺ cDCs. Cell surface was stained with anti-CD11c, anti-NK1.1, anti-PDCA1, anti-CD4, and anti-CD8 α . Cell interior was stained by anti-TLR7. The ratio of mean fluorescence intensity was calculated and shown by graph. Representative data are shown by density plot. **(B)** IL-6 production from CD8 α ⁺ cDCs. Cells were collected by cell sorter and stimulated with TLR7 ligand. At least four mice sex and age matched were used (A). Three independent experiments were performed. CD8 α ⁺ cDCs were stimulated in triplicated wells, and the mean SD was shown (B). ** $p < 0.01$, *** $p < 0.001$.

Acknowledgments

We thank Prof. Y. Iwakura for providing *lfnar1*^{-/-} and *lfnar1*^{+/+} mice and T. Hayashi who helped with some of the experiments on this work.

Disclosures

The authors have no financial conflicts of interest.

References

- Kawai, T., and S. Akira. 2010. The role of pattern-recognition receptors in innate immunity: update on Toll-like receptors. *Nat. Immunol.* 11: 373–384.
- Blasius, A. L., and B. Beutler. 2010. Intracellular Toll-like receptors. *Immunity* 32: 305–315.
- Takeuchi, O., and S. Akira. 2010. Pattern recognition receptors and inflammation. *Cell* 140: 805–820.
- Miyake, K., and T. Kaisho. 2014. Homeostatic inflammation in innate immunity. *Curr. Opin. Immunol.* 30: 85–90.
- Krieg, A. M., and J. Vollmer. 2007. Toll-like receptors 7, 8, and 9: linking innate immunity to autoimmunity. *Immunol. Rev.* 220: 251–269.
- Deane, J. A., P. Pisitkun, R. S. Barrett, L. Feigenbaum, T. Town, J. M. Ward, R. A. Flavell, and S. Bolland. 2007. Control of Toll-like receptor 7 expression is essential to restrict autoimmunity and dendritic cell proliferation. *Immunity* 27: 801–810.
- Santiago-Raber, M. L., S. Kikuchi, P. Borel, S. Uematsu, S. Akira, B. L. Kotzin, and S. Izui. 2008. Evidence for genes in addition to Tlr7 in the Yaa translocation linked with acceleration of systemic lupus erythematosus. *J. Immunol.* 181: 1556–1562.
- Pisitkun, P., J. A. Deane, M. J. Difilippantonio, T. Tarasenko, A. B. Satterthwaite, and S. Bolland. 2006. Autoreactive B cell responses to RNA-related antigens due to TLR7 gene duplication. *Science* 312: 1669–1672.
- Christensen, S. R., J. Shupe, K. Nickerson, M. Kashgarian, R. A. Flavell, and M. J. Shlomchik. 2006. Toll-like receptor 7 and TLR9 dictate autoantibody specificity and have opposing inflammatory and regulatory roles in a murine model of lupus. *Immunity* 25: 417–428.
- Fukui, R., and K. Miyake. 2012. Controlling systems of nucleic acid sensing-TLRs restrict homeostatic inflammation. *Exp. Cell Res.* 318: 1461–1466.
- Fukui, R., S. Saitoh, F. Matsumoto, H. Kozuka-Hata, M. Oyama, K. Tabeta, B. Beutler, and K. Miyake. 2009. UNC93B1 biases Toll-like receptor responses to nucleic acid in dendritic cells toward DNA- but against RNA-sensing. *J. Exp. Med.* 206: 1339–1350.
- Brinkmann, M. M., E. Spooner, K. Hoebe, B. Beutler, H. L. Ploegh, and Y. M. Kim. 2007. The interaction between the ER membrane protein UNC93B and TLR3, 7, and 9 is crucial for TLR signaling. *J. Cell Biol.* 177: 265–275.
- Kim, Y. M., M. M. Brinkmann, M. E. Paquet, and H. L. Ploegh. 2008. UNC93B1 delivers nucleotide-sensing Toll-like receptors to endolysosomes. *Nature* 452: 234–238.
- Latz, E., A. Schoenemeyer, A. Visintin, K. A. Fitzgerald, B. G. Monks, C. F. Knetter, E. Lien, N. J. Nilsen, T. Espevik, and D. T. Golenbock. 2004.

- TLR9 signals after translocating from the ER to CpG DNA in the lysosome. *Nat. Immunol.* 5: 190–198.
15. Tabeta, K., K. Hoebe, E. M. Janssen, X. Du, P. Georgel, K. Crozat, S. Mudd, N. Mann, S. Sovath, J. Goode, et al. 2006. The Unc93b1 mutation 3d disrupts exogenous antigen presentation and signaling via Toll-like receptors 3, 7 and 9. *Nat. Immunol.* 7: 156–164.
 16. Fukui, R., S. Saitoh, A. Kanno, M. Onji, T. Shibata, A. Ito, M. Onji, M. Matsumoto, S. Akira, N. Yoshida, and K. Miyake. 2011. Unc93B1 restricts systemic lethal inflammation by orchestrating Toll-like receptor 7 and 9 trafficking. *Immunity* 35: 69–81.
 17. Raphael, L., S. Nalawade, T. N. Eagar, and T. G. Forsthuber. 2015. T cell subsets and their signature cytokines in autoimmune and inflammatory diseases. *Cytokine* 74: 5–17.
 18. Mills, K. H. 2011. TLR-dependent T cell activation in autoimmunity. *Nat. Rev. Immunol.* 11: 807–822.
 19. Jin, B., T. Sun, X. H. Yu, Y. X. Yang, and A. E. Yeo. 2012. The effects of TLR activation on T-cell development and differentiation. *Clin. Dev. Immunol.* 2012: 836485.
 20. Yang, Q., B. Wang, H. Yu, Y. Zhu, X. Wang, H. Jiang, C. Wang, J. Peng, and M. Hou. 2011. TLR7 promotes Th1 polarization in immune thrombocytopenia. *Thromb. Res.* 128: 237–242.
 21. Green, N. M., A. Laws, K. Kiefer, L. Busconi, Y. M. Kim, M. M. Brinkmann, E. H. Trail, K. Yasuda, S. R. Christensen, M. J. Shlomchik, et al. 2009. Murine B cell response to TLR7 ligands depends on an IFN- β feedback loop. *J. Immunol.* 183: 1569–1576.
 22. Bekerdejian-Ding, I. B., M. Wagner, V. Hornung, T. Giese, M. Schnurr, S. Endres, and G. Hartmann. 2005. Plasmacytoid dendritic cells control TLR7 sensitivity of naive B cells via type I IFN. *J. Immunol.* 174: 4043–4050.
 23. Kanno, A., C. Yamamoto, M. Onji, R. Fukui, S. Saitoh, Y. Motoi, T. Shibata, F. Matsumoto, T. Muta, and K. Miyake. 2013. Essential role for Toll-like receptor 7 (TLR7)-unique cysteines in an intramolecular disulfide bond, proteolytic cleavage and RNA sensing. *Int. Immunol.* 25: 413–422.
 24. Rose, S., A. Misharin, and H. Perlman. 2012. A novel Ly6C/Ly6G-based strategy to analyze the mouse splenic myeloid compartment. *Cytometry A* 81: 343–350.
 25. Chiassone, L., J. Chaix, N. Fuseri, C. Roth, E. Vivier, and T. Walzer. 2009. Maturation of mouse NK cells is a 4-stage developmental program. *Blood* 113: 5488–5496.
 26. Matsushita, K., O. Takeuchi, D. M. Standley, Y. Kumagai, T. Kawagoe, T. Miyake, T. Satoh, H. Kato, T. Tsujimura, H. Nakamura, and S. Akira. 2009. Zc3h12a is an RNase essential for controlling immune responses by regulating mRNA decay. *Nature* 458: 1185–1190.
 27. Santiago-Raber, M. L., H. Amano, E. Amano, L. Fossati-Jimack, L. K. Swee, A. Rolink, and S. Izui. 2010. Evidence that Yaa-induced loss of marginal zone B cells is a result of dendritic cell-mediated enhanced activation. *J. Autoimmun.* 34: 349–355.
 28. Ahuja, A., J. Shupe, R. Dunn, M. Kashgarian, M. R. Kehry, and M. J. Shlomchik. 2007. Depletion of B cells in murine lupus: efficacy and resistance. *J. Immunol.* 179: 3351–3361.
 29. Chan, O., and M. J. Shlomchik. 1998. A new role for B cells in systemic autoimmunity: B cells promote spontaneous T cell activation in MRL-lpr/lpr mice. *J. Immunol.* 160: 51–59.
 30. Nickerson, K. M., J. L. Cullen, M. Kashgarian, and M. J. Shlomchik. 2013. Exacerbated autoimmunity in the absence of TLR9 in MRL.Fas(lpr) mice depends on Ifnar1. *J. Immunol.* 190: 3889–3894.
 31. Vremec, D., J. Pooley, H. Hochrein, L. Wu, and K. Shortman. 2000. CD4 and CD8 expression by dendritic cell subtypes in mouse thymus and spleen. *J. Immunol.* 164: 2978–2986.
 32. Coquerelle, C., and M. Moser. 2010. DC subsets in positive and negative regulation of immunity. *Immunol. Rev.* 234: 317–334.
 33. Hochrein, H., K. Shortman, D. Vremec, B. Scott, P. Hertzog, and M. O’Keeffe. 2001. Differential production of IL-12, IFN- α , and IFN- γ by mouse dendritic cell subsets. *J. Immunol.* 166: 5448–5455.
 34. Proietto, A. I., M. O’Keeffe, K. Gartlan, M. D. Wright, K. Shortman, L. Wu, and M. H. Lahoud. 2004. Differential production of inflammatory chemokines by murine dendritic cell subsets. *Immunobiology* 209: 163–172.
 35. Bialecki, E., E. Macho Fernandez, S. Ivanov, C. Paget, J. Fontaine, F. Rodriguez, L. Lebeau, C. Ehret, B. Frisch, F. Trottein, and C. Faveeuw. 2011. Spleen-resident CD4⁺ and CD4⁺CD8 α ⁺ dendritic cell subsets differ in their ability to prime invariant natural killer T lymphocytes. *PLoS One* 6: e26919.
 36. King, I. L., E. Amiel, M. Tighe, K. Mohrs, N. Veerapen, G. Besra, M. Mohrs, and E. A. Leadbetter. 2013. The mechanism of splenic invariant NKT cell activation dictates localization in vivo. *J. Immunol.* 191: 572–582.
 37. Vomhof-DeKrey, E. E., J. Yates, and E. A. Leadbetter. 2014. Invariant NKT cells provide innate and adaptive help for B cells. *Curr. Opin. Immunol.* 28: 12–17.
 38. Bialecki, E., C. Paget, J. Fontaine, M. Capron, F. Trottein, and C. Faveeuw. 2009. Role of marginal zone B lymphocytes in invariant NKT cell activation. *J. Immunol.* 182: 6105–6113.
 39. Enoksson, S. L., E. K. Grasset, T. Hägglöf, N. Mattsson, Y. Kaiser, S. Gabriellson, T. L. McGaha, A. Scheynius, and M. C. Karlsson. 2011. The inflammatory cytokine IL-18 induces self-reactive innate antibody responses regulated by natural killer T cells. *Proc. Natl. Acad. Sci. USA* 108: E1399–E1407.
 40. Wermeling, F., S. M. Lind, E. D. Jordö, S. L. Cardell, and M. C. Karlsson. 2010. Invariant NKT cells limit activation of autoreactive CD1d-positive B cells. *J. Exp. Med.* 207: 943–952.
 41. Green, N. M., and A. Marshak-Rothstein. 2011. Toll-like receptor driven B cell activation in the induction of systemic autoimmunity. *Semin. Immunol.* 23: 106–112.
 42. Preble, O. T., R. J. Black, R. M. Friedman, J. H. Klippel, and J. Vilcek. 1982. Systemic lupus erythematosus: presence in human serum of an unusual acid-labile leukocyte interferon. *Science* 216: 429–431.
 43. Olsen, N. J., and D. R. Karp. 2014. Autoantibodies and SLE: the threshold for disease. *Nat. Rev. Rheumatol.* 10: 181–186.
 44. Meroni, P. L., and P. H. Schur. 2010. ANA screening: an old test with new recommendations. *Ann. Rheum. Dis.* 69: 1420–1422.
 45. Rönnblom, L., and M. L. Eloranta. 2013. The interferon signature in autoimmune diseases. *Curr. Opin. Rheumatol.* 25: 248–253.
 46. Baechler, E. C., F. M. Batliwalla, G. Karypis, P. M. Gaffney, W. A. Ortmann, K. J. Espe, K. B. Shark, W. J. Grande, K. M. Hughes, V. Kapur, et al. 2003. Interferon-inducible gene expression signature in peripheral blood cells of patients with severe lupus. *Proc. Natl. Acad. Sci. USA* 100: 2610–2615.
 47. Ramirez-Ortiz, Z. G., A. Prasad, J. W. Griffith, W. F. Pendergraft, III, G. S. Cowley, D. E. Root, M. Tai, A. D. Luster, J. El Khoury, N. Hacohen, and T. K. Means. 2015. The receptor TREML4 amplifies TLR7-mediated signaling during antiviral responses and autoimmunity. *Nat. Immunol.* 16: 495–504.
 48. Christensen, S. R., M. Kashgarian, L. Alexopoulou, R. A. Flavell, S. Akira, and M. J. Shlomchik. 2005. Toll-like receptor 9 controls anti-DNA autoantibody production in murine lupus. *J. Exp. Med.* 202: 321–331.
 49. Lian, Z. X., K. Kikuchi, G. X. Yang, A. A. Ansari, S. Ikehara, and M. E. Gershwin. 2004. Expansion of bone marrow IFN- α -producing dendritic cells in New Zealand Black (NZB) mice: high level expression of TLR9 and secretion of IFN- α in NZB bone marrow. *J. Immunol.* 173: 5283–5289.
 50. Santiago-Raber, M. L., R. Baccala, K. M. Haraldsson, D. Choubey, T. A. Stewart, D. H. Kono, and A. N. Theofilopoulos. 2003. Type-I interferon receptor deficiency reduces lupus-like disease in NZB mice. *J. Exp. Med.* 197: 777–788.
 51. Ivashkiv, L. B., and L. T. Donlin. 2014. Regulation of type I interferon responses. *Nat. Rev. Immunol.* 14: 36–49.
 52. Roh, Y. S., S. Park, J. W. Kim, C. W. Lim, E. Seki, and B. Kim. 2014. Toll-like receptor 7-mediated type I interferon signaling prevents cholestasis- and hepatotoxin-induced liver fibrosis. *Hepatology* 60: 237–249.
 53. de Weerd, N. A., S. A. Samarajiwa, and P. J. Hertzog. 2007. Type I interferon receptors: biochemistry and biological functions. *J. Biol. Chem.* 282: 20053–20057.
 54. Thomas, C., I. Moraga, D. Levin, P. O. Krutzik, Y. Podoplelova, A. Trejo, C. Lee, G. Yarden, S. E. Vleck, J. S. Glenn, et al. 2011. Structural linkage between ligand discrimination and receptor activation by type I interferons. *Cell* 146: 621–632.